Non-Darcy Flow Behavior near High-Flux Injection Wells in Porous and Fractured Formations

Yu-Shu Wu
Earth Sciences Division
Lawrence Berkeley National Laboratory
Berkeley CA 94720, USA

Abstract

This paper presents a study of non-Darcy fluid flow through porous and fractured rock, which may occur near wells during high-flux injection of waste fluids into underground formations. Both numerical and analytical models are used in this study. General non-Darcy flow is described using the *Forchheimer* equation, implemented in a three-dimensional, multiphase flow reservoir simulator. The non-Darcy flow through a fractured reservoir is handled using a general dual continuum approach, covering commonly used conceptual models, such as double porosity, dual permeability, explicit fracture, etc. Under single-phase flow conditions, an approximate analytical solution, as an extension of the Warren-Root solution, is discussed.

The objectives of this study are (1) to obtain insights into the effect of non-Darcy flow on transient pressure behavior through porous and fractured reservoirs and (2) to provide type curves for well test analyses of non-Darcy flow wells. The type curves generated include various types of drawdown, injection, and buildup tests with non-Darcy flow occurring in porous and fractured reservoirs. In addition, non-Darcy flow into partially penetrating wells is also considered. The transient-pressure type curves for flow in fractured reservoirs are based on the double-porosity model. Type curves provided in this work for non-Darcy flow in porous and fractured reservoirs will find their applications in well test interpretation using a type-curve matching technique.

1. Introduction

Darcy's law has been used exclusively in studies of porous-medium phenomena. However, high-velocity non-Darcy flow occurs in many cases involving subsurface flow systems, such as in the flow near high-flux wells during oil or gas production, water pumping, and liquid waste injection. Theoretical, field, and experimental studies on non-Darcy flow in porous media have been performed, most of which have been focused on single-phase flow conditions that pertain to the oil and gas industry (e.g., *Tek et al*., 1962; *Swift and Kiel*, 1962; *Lee et al.* 1987). Other researchers have devoted their efforts to finding and validating correlations of non-Darcy flow coefficients [*e.g., Liu et al*., 1995].

In studies of non-Darcy flow through porous media, the *Forchheimer* equation has been generally used to describe single-phase non-Darcy flow. Several studies in the literature extend the *Forchheimer* equation to multiphase flow and provide equations for correlating non-Darcy flow coefficients under multiphase conditions [*Evans et al*., 1987; *Evans and Evans*, 1988; *Liu et al*.,

1995; *Wu* 2001]. A general numerical method has been recently developed in modeling single-phase and multiphase non-Darcy flow in multidimensional porous and fractured reservoirs [*Wu* 2002a]. This numerical model incorporates the extended *Forchheimer* equation using an integral finite-difference or a control-volume-numerical-discretization scheme, and implements an extended dual-continuum approach (such as double- or multiple-porosity, or dual-permeability method) for simulating non-Darcy fracture-matrix flow in a fractured medium. In addition, an approximate analytical solution is also obtained for analyzing non-Darcy well flow behavior through fractured reservoirs [*Wu*, 2002b].

The objectives of this study are (1) to obtain insights into non-Darcy flow on transient pressure behavior through porous and fractured reservoirs and (2) to provide type curves for well test analyses of non-Darcy flow wells. The type curves generated include cases of drawdown, injection, and buildup tests with non-Darcy flow occurring in porous and fractured reservoirs. In addition, non-Darcy flow into partially penetrating wells is also considered. The transient pressure type curves for flow in fractured reservoirs are based on the double-porosity model. The type curves provided in this work will find their applications in interpreting well tests of non-Darcy flow in porous and fractured reservoirs using a type-curve matching technique.

2. Mathematical Model and Numerical Formulation

A multiphase system in a porous or fractured aquifer is assumed to be composed of three phases: NAPL (oil), gas (air), and water. For simplicity, the three fluid components, water, NAPL, and gas, are assumed to be present only in their associated phases, with single-phase flow regarded as a special case of multiphase flow here. Each phase flows in response to pressure, gravitational, and capillary forces according to the multiphase extension of the *Forchheimer* equation for non-Darcy flow:

$$\frac{\partial}{\partial t}(\phi S_f \rho_f) = -\nabla \bullet (\rho_f \mathbf{v}_f) + q_f \qquad (2.1)$$

where ρ_f is the density of fluid f (f = w for water, f = n for NAPL or oil, and f = g for gas); $\mathbf{v}_f$ is the Darcy (or volumetric) velocity of fluid f; S_f is the saturation of fluid f; ϕ is the effective porosity of formation; t is time; and q_f is the sink/source term of phase (component) f per unit volume of formation, representing mass exchange through injection/production wells or resulting from fracture-matrix interactions.

Volumetric flow rate (namely Darcy velocity in the case of Darcy flow) for non-Darcy flow of each fluid may be described using the multiphase extension of the *Forchheimer* equation [*Evans and Evans*, 1988; *Liu et al.,* 1995; *Katz and Lee*, 1990]:

$$-(\nabla P_f - \rho_f \mathbf{g}) = \frac{\mu_f}{k_{rf}} k \mathbf{v}_f + \beta_f \rho_f \mathbf{v}_f |\mathbf{v}_f| \qquad (2.2)$$

where P_f is the pressure of phase f; $\mathbf{g}$ is the gravitational constant vector; μ_f is the dynamic viscosity of fluid f, k is the absolute/intrinsic permeability of the formation; k_{rf} is relative

permeability to phase f; and β_f is the effective non-Darcy flow coefficient with a unit m^{-1} for fluid f under multiphase flow conditions [*Evans and Evans*, 1988].

Equation (2.1), the mass-balance governing equation for three phases needs to be supplemented with constitutive equations, which express all the secondary variables and parameters as functions of a set of primary thermodynamic variables of interest. Here, we borrow relative permeability and capillary pressure relations, and other correlations such as density and viscosity, from the multiphase Darcy flow model to complete the problem description.

The additional nonlinearity introduced by non-Darcy flow to the governing equations makes it in general necessary to use a numerical approach. Equation (2.1) can be discretized in space using an integral finite-difference or control-volume finite-element scheme for a porous and/or fractured medium [*Wu,* 2002a]. The time discretization is carried out with a backward, first-order, finite-difference scheme. The discrete nonlinear equations for water, NAPL, and gas flow at Node i are written as follows:

$$\left\{\left(\phi\, S_f \rho_f\right)_i^{n+1} - \left(\phi\, S_f \rho_f\right)_i^{n}\right\}\frac{V_i}{\Delta t} = \sum_{j\in\eta_i}\left(F_f\right)_{ij}^{n+1} + Q_{fi}^{n+1} \tag{2.3}$$

where n denotes the previous time level; n+1 is the current time level; V_i is the volume of element i (porous or fractured block); Δt is the time step size; and η_i contains the set of neighboring elements (j), porous or fractured block, to which element i is directly connected. F_f is a mass flow term between elements i and j, defined [when Equation (2.2) is used] as

$$F_f = \frac{A_{ij}}{2\left(k\beta_f\right)_{ij+1/2}}\left\{-\frac{1}{\lambda_f} + \left[\left(\frac{1}{\lambda_f}\right)^2 - \gamma_{ij}\left(\psi_{fj} - \psi_{fi}\right)\right]^{1/2}\right\} \tag{2.4}$$

where subscript ij+1/2 denotes a proper averaging of properties at the interface between the two elements and A_{ij} is the common interface area between connected elements i and j. The mobility of phase f is defined as

$$\lambda_f = \frac{k_{rf}}{\mu_f} \tag{2.5}$$

and the flow potential term is

$$\psi_{fi} = P_{fi} - \rho_{ij+1/2} g D_i \tag{2.6}$$

where D_i is the depth to the center of element i. The mass sink/source term at element i, Q_{fi} for phase f, is defined as

$$Q_{fi} = q_{fi} V_i \tag{2.7}$$

In Equation (2.4), the transmissivity of flow terms is defined (if the integral finite-difference scheme is used) as,

$$\gamma_{ij} = \frac{4\left(k^2 \rho_f \beta_f\right)_{ij+1/2}}{d_i + d_j}, \tag{2.8}$$

where d_i is the distance from the center of element i to the interface between elements i and j.

In the model formulation, absolute permeability, relative permeability, and the effective non-Darcy flow coefficient are all considered as flow properties of the porous media and need to be averaged between connected elements in calculating the mass-flow terms. In general, absolute permeability is harmonically weighted along the connection between elements i and j, and relative permeability and non-Darcy flow coefficients are both upstream weighted. Then, the nonlinear, discrete Equation (2.3) is solved using a Newton/Raphson iteration.

The technique used for handling non-Darcy flow through fractured rock follows the dual-continuum methodology [*Warren and Root*, 1963; *Pruess and Narasimhan*, 1985; *Wu,* 2002a]. The method treats fracture-matrix interactions with a multicontinuum numerical approach, including the double- or multiporosity method, the dual-permeability method, and the more general "multiple interacting continua" (MINC) method. The non-Darcy flow formulation, Equation (2.1) or (2.3) is applicable to both singlecontinuum and multicontinuum media. Using the dual-continuum concept, Equation (2.1) or (2.3) can be used to describe single-phase and multiphase flow, respectively, both in fractures and inside matrix blocks when dealing with fractured reservoirs. Special attention needs to be paid to treating fracture-matrix flow terms with Equations (2.3) and (2.4) for estimation of mass exchange at fracture-matrix interfaces using a double-porosity approach. In particular, *Wu* [2002a] has shown that for the double-porosity or nested discretizations, the characteristic length of non-Darcy flow distance between fractures and matrix crossing the interface may be approximated using the results for Darcy flow [*Warren and Root*, 1965; *Pruess*, 1983]. The flow between fractures and matrix is still evaluated using Equation (2.4), however, the transmissivity for the fracture/matrix flow is then given by

$$\gamma_{ij} = \frac{4\left(k_m^2 \rho_f \beta_f\right)_{ij+1/2}}{l_{fm}}, \qquad (2.9)$$

where k_m is matrix permeability, and l_{fm} is the characteristic distance for flow crossing fracture-matrix interfaces (Table 4.1, *Wu*, 2002a)

In modeling flow through a fractured rock using the numerical formulation of this work, what a modeler needs to do is essentially to figure out how to generate a grid that represents both the fracture and matrix systems. Several fracture-matrix subgridding schemes exist for designing different meshes for different fracture-matrix conceptual models [*Pruess*, 1983]. Once a proper mesh of a fracture-matrix system is generated, fracture and matrix blocks are specified to represent fracture or matrix domains, separately. Formally, they are treated in exactly the same way in the solution of the discretized model. However, physically consistent fracture and matrix properties and modeling conditions must be appropriately specified for fracture and matrix systems, respectively.

3. Dimensionless Variable and Analytical Solution

Let us define the following group of dimensionless variables [*Earlougher*, 1977; *Warren and Root*, 1963]: the dimensionless radius is

$$r_D = \frac{r}{r_w} \tag{3.1}$$

with r being the radial coordinate or distance and r_w a well radius. The dimensionless time is

$$t_D = \frac{k\ t}{\mu r_w^2 \phi C} \tag{3.2a}$$

for porous formation,

$$t_D = \frac{k_f t}{\mu r_w^2 \left(\phi_m C_m + \phi_f C_f\right)} \tag{3.2b}$$

for fractured formation. In Equation (3.2), k_f is fracture absolute permeability in fractured formation, C is compressibility, and subscripts, m and f denote matrix and fracture, respectively. The dimensionless non-Darcy flow coefficient is

$$\beta_D = \frac{k q_m \beta}{2\pi r_w h \mu} \tag{3.3a}$$

for porous formation, and

$$\beta_D = \frac{k_f q_m \beta}{2\pi r_w h \mu} \tag{3.3b}$$

for fractured formation. and the dimensionless fracture pressure is

$$P_D = \frac{P_i - P_w(t)}{\frac{q\ \mu}{2\pi k_f h}} \tag{3.4}$$

where P_i is the initial pressure of formation, a constant, and $P_w(t)$ is the well pressure, a function of time. Note that in Equation (3.3), q_m is a mass production or injection rate, treated as a constant.

In addition, Warren and Root define two more dimensionless parameters to characterize double-porosity flow behavior. The first one is the ratio of fracture porosity-compressibility to the total system porosity-compressibility product as:

$$\omega = \frac{\phi_f C_f}{\phi_m C_m + \phi_f C_f} \tag{3.5}$$

and the second is the interporosity flow parameter:

$$\lambda = \frac{\alpha r_w^2 k_m}{k_f}; \tag{3.6}$$

with α being a shape factor of rock matrix blocks.

An approximate analytical solution for transient non-Darcy flow in a fractured medium is derived [*Wu*, 2002b] as a superposition of the *Warren-Root* solution [1963] and the non-Darcy flow coefficient:

$$P_D(r_D = 1, t_D) = \beta_D + \frac{1}{2}\left[\ln t_D + 0.80907 + E_i\left(-\frac{\lambda t_D}{\omega(1-\omega)}\right) - E_i\left(-\frac{\lambda t_D}{(1-\omega)}\right)\right] \quad (3.7)$$

This approximate solution has been shown to be very accurate for non-Darcy flow through normal double-porosity fractured media [*Wu*, 2002b].

4. Type Curves of Non-Darcy Flow

In this section, we present several applications and discuss single-phase, non-Darcy flow behavior. In addition, we provide several commonly used dimensionless pressures or type curves for non-Darcy-flow well-test analyses, including:

(1) Pressure drawdown and buildup analyses
(2) Effects of finite boundaries for reservoirs
(3) Pressure draw-down in fractured reservoirs
(4) Pressure responses in partially penetrating wells of porous and fractured reservoirs

These application examples deal with single-phase slightly compressible fluid transient flow. In addition, type curves of non-Darcy flow through a single well are generated using numerical solutions for single-phase, slightly compressible non-Darcy fluid flow in infinite-acting or finite-acting reservoirs.

Pressure Drawdown and Buildup

This example deals with non-Darcy flow through an infinite-acting reservoir. The flow is approximated by a one-dimensional, radially symmetrical formation in the numerical model, with an outer boundary radius of 5×10^6 (m), discretized into a one-dimensional grid of 3,100 gridblocks in logarithmic scale. Initially, the system is undisturbed and at constant pressure. A fully penetrating production well, represented by a well element, starts pumping at t = 0, specified at a constant water-pumping rate. Input parameters for this problem are presented in Table 1.

Figure 1 shows a set of type curves for pressure drawdown, calculated by the numerical model in terms of dimensionless pressure versus dimensionless time. As shown here, the non-Darcy flow coefficient is a very important and sensitive parameter for pressure drawdown plots. Therefore, the figure indicates that the non-Darcy flow coefficient can be effectively estimated using the type curves with the traditional type-curve matching approach due to its sensitivity.

Figure 2 presents simulated pressure drawdown and buildup curves, in which the well is pumped for one day only and then shut off. The well pressure variations during the entire pumping and shut-in period, as shown in Figure 2, indicate that pressure buildup is insensitive to the values of

non-Darcy flow coefficients, compared to drawdown in pumping periods. This insensitivity results from the rapid reduction in flow velocity near the well after a well is shut off and non-Darcy flow effects become ineligible. Many additional modeling investigations have verified this observation. Therefore, pressure-buildup tests are not suitable for estimating non-Darcy flow coefficients. On the other hand, the pressure-buildup method following non-Darcy flow pumping tests will be a good way to determine permeability values without significant non-Darcy flow effect.

Effects of Finite Reservoir Boundaries

Boundary effects or well interference in finite, developed reservoirs will show up in well tests sooner or later. Two types of boundary conditions, closed and constant pressure conditions, are commonly used to approximate the effects of finite reservoir/well boundaries. A finite flow system and parameters for finite systems are similar to those above. Only two finite radial systems with outer boundary radii (r_e =1,000 and 10,000 m) are considered. Figures 3 and 4 show dimensionless pressure drawdown curves, for closed and constant-pressure boundaries as well as the two radii. For a smaller, finite, formation system with r_e = 1,000 m, Figure 3 shows that significant boundary effects occur at about dimensionless time $t_D = 10^8$ (1 day in real time), at which the well pressure responses deviate from the infinite-acting solution (say, the Theis solution for small non-Darcy flow coefficients). For the larger system with r_e = 10,000 m, boundary effects are very similar; but show up much later (Figure 4).

Non-Darcy Flow in Fractured Media

This problem reflects non-Darcy flow through a fractured reservoir. Fracture-matrix formation is described using the *Warren* and *Root* double-porosity model [*Wu*, 2002a]. The physical flow model is that of typical transient flow towards a well that fully penetrates a radially infinite horizontal, uniform, fractured reservoir. In numerical modeling for comparison, a radially finite reservoir ($r_e = 5 \times 10^6$ m) is used and discretized into a one-dimensional (primary) grid. The r-distance of 5×10^6 m is subdivided into 3,100 intervals in a logarithmic scale. A double-porosity mesh is generated from the primary grid, in which a three-dimensional fracture network and cubic matrix blocks are used. The uniform matrix block size is $1 \times 1 \times 1$ m, and fracture permeability and aperture are correlated by the cubic law. Input parameters are given in Table 2.

Figure 5 shows a comparison of the numerical modeling results and the approximate analytical solution (3.7) with different dimensionless non-Darcy flow coefficients. The two characteristic parameters for these cases are $\lambda = 6\times10^{-5}$ and $\omega = 2\times10^{-3}$, from the parameters used as listed in Table 2. Note that the values of these two parameters are within a typical range of double-porosity flow behavior as discussed by Warren and Root. Figure 5 shows excellent agreement between the analytical (circled-symbol curves, labeled as $P_{D,WR}+ \beta_D$) and numerical (solid-line curves) solutions, except at earlier times ($t_D < 100$) or for large non-Darcy flow coefficients ($\beta_D > 10$).

For non-Darcy flow into a well from an infinite fractured system, well pressure type curves shown in

semi-log plots of Figure 5. The type curves in the figure show that well (fracture) pressures are extremely sensitive to the value of non-Darcy flow coefficients; therefore, well pumping tests will help to determine this constant in a fractured reservoir. Furthermore, Figure 5 indicates that the effects of non-Darcy flow on early transient pressure responses are very strong, such that the first semi-log straight lines may not develop when non-Darcy flow is involved in a fracture reservoir.

Non-Darcy Flow with Partial Penetrating Wells

Here, non-Darcy flow is considered occurring in a partially penetrating well from an infinite-acting, homogeneous, isotropic, porous or fractured reservoir. Flow near a partially penetrating production well is three-dimensional towards the wellbore and it is can be handled mathematically using a 2-D, axially-symmetrical (r-z) grid. In the numerical model, the infinite-acting reservoir is approximated by a 2-D, radially symmetrical reservoir with an outer boundary radius ($r = 1 \times 10^7$ m) and a thickness of 10 m in the vertical, z-direction. The system is discretized into a 2-D grid of 1,000 divisions in the r direction, using a logarithmic scale and five uniform grid layers in the z direction for the porous reservoir. For the fractured flow example, the single-porosity, porous reservoir grid is further processed into a double-porosity grid using the MINC technology. Initially, the two single-phase systems are both at vertical-gravity equilibrium. Partially penetrating wells with a percentage of wellbore completion are represented by single-well elements, and the results are compared.

The parameters for the porous reservoir are those given in Table 1, and the fractured-reservoir properties are given in Table 2. The fractured reservoir is handled using the double-porosity model. Two type-curves for pressure drawdown, calculated in terms of dimensionless pressure versus dimensionless time, are shown in Figures 6 and 7, respectively, for the porous and fractured reservoirs. Figures 6 and 7 show the significant impact of well-penetration percentage on well pressure behavior in both the porous medium and fractured reservoirs. As completed well screen lengths decrease (i.e., as wellbore penetration or open-screen length becomes smaller), the flow resistance and pressure drops at the well increase significantly to maintain the same production rates. We could expect a larger impact of well partial penetration on non-Darcy flow regime near a well than on Darcy flow, because of higher flow rates or large non-Darcy flow effects near wellbore. However, comparison of the straight lines developed in the type curves at late times (Figures 6 and 7) indicates that the same pseudo-skin concept [*Earlougher*, 1977] may also be applicable to analyzing partial penetration effects of non-Darcy flow at wells.

5. Summary and Conclusions

This paper presents a theoretical study of non-Darcy flow behavior through porous and fractured rock, which may occur near pumping or production wells during high-flux injection of waste fluids into underground formations. Both numerical and analytical solutions are used, with non-Darcy flow simulated using the *Forchheimer* equation and a three-dimensional, multiphase flow reservoir simulator. Non-Darcy flow through a fractured reservoir is handled using a general dual-continuum approach, covering commonly used conceptual models, such as double porosity, dual

permeability, and explicit fracture models.

Using numerical simulation results, we discuss fundamental non-Darcy flow behavior for transient pressures in porous and fractured reservoirs. In particular, we provide a number of dimensionless type curves for well test analyses of non-Darcy flow wells. The type curves generated include various types of drawdown, injection, and buildup tests with non-Darcy flow occurring in porous and fractured reservoirs. In addition, non-Darcy flow into partially penetrating wells is also considered. The type curves provided in this work for non-Darcy flow in porous and fractured reservoirs can be used in well test interpretations using a type-curve matching technique.

Acknowledgement

The author is indebted to Guoxiang Zhang and Dan Hawkes for their careful and critical review of this manuscript. This work was supported in part by the Assistant Secretary for Energy Efficiency and Renewable Energy, Office of Geothermal and Wind Technologies of the U.S. Department of Energy. The support is provided to Berkeley Lab through the U.S. Department of Energy Contract No. DE-AC03-76SF00098

References

Earlougher, R. C. Jr., *Advances in Well Test Analysis*, SPE Monograph, Vol. 5, SPE of AIME, Dallas, 1977.

Evans, E. V. and R. D. Evans, Influence of an immobile or mobile saturation on non-Darcy compressible flow of real gases in propped fractures, *J. Petroleum Technology,* Vol. 40, No. 10, pp.1343-1351, 1988.

Evans, R. D., C. S. Hudson and J. E. Greenlee, The effect of an immobile liquid saturation on the non-Darcy flow coefficient in porous media, *J. SPE Production Engineering, Trans*. AIME, Vol. 283, pp.331-338, 1987.

Katz, D. L. and R. L. Lee, *Natural Gas Engineering, Production and Storage*, Chemical Engineering Series, McGraw-Hill Book Co. Inc., New York, 1990.

Lee, R. L., R. W. Logan and M. R. Tek: "Effetcs of turbulence on transient flow of real gas through porous media," *SPE Formation Evaluation*, pp.108-120, 1987.

Liu, X., F. Civan and R. D. Evans, Correlations of the non-Darcy flow coefficient, *J. Canadian Petroleum Technology,* Vol. 34, No. 10, pp.50-54, 1995.

Pruess, K. and Narasimhan, T. N., A practical method for modeling fluid and heat flow in fractured porous media, *Soc. Pet. Eng. J., 25,* pp.14-26, 1985.

Pruess, K., GMINC - A mesh generator for flow simulations in fractured reservoirs, Report LBL-15227, Berkeley, California: Lawrence Berkeley National Laboratory, 1983.

Swift, G. W. and O. G. Kiel, The prediction of gas-well performance including the effects of non-Darcy flow, *J. Petroleum Technology, Trans*. AIME, Vol. 222, pp.791-798, 1962.

Tek, M. R., K. H. Coats and D. L. Katz, The effects of turbulence on flow of natural gas through porous reservoirs, *J. Petroleum Technology, Tran.s* AIME, Vol. 222, pp.799-806, 1962.

Warren, J.E., and P. J. Root, The behavior of naturally fractured reservoirs, *Soc. Pet. Eng. J., Trans., AIME*, pp.245-255, 228, 1963.

Wu, Y. S., Numerical Simulation of Single-Phase and Multiphase Non-Darcy Flow in Porous and Fractured Reservoirs, LBNL-45855, *Transport In Porous Media*, Vol. 49, No. 2, pp.209-240, 2002a.

Wu, Y. S., An Approximate Analytical Solution for Non-Darcy Flow in Fractured Media, LBNL-48197, Vol.38, No. 3, *Water Resources Research*, pp.5-1-5-7, 2002b.

Wu, Y. S., Non-Darcy Displacement of Immiscibel Fluids in Porous Media, LBNL-45228, Vol. 37, No. 12, *Water Resources Research*, pp. 2943-2950, December 2001.

Table 1. Parameters for the pressure drawdown and buildup analysis.

Parameter	Value	Unit
Initial Pressure	$P_i = 10$	Bar
Initial Porosity	$\phi_i = 0.20$	
Reference Fluid Density	$\rho_i = 1{,}000$	kg/m^3
Formation Thickness	h=10	m
Fluid Viscosity	$\mu = 1\times10^{-3}$	Pa•s
Fluid Compressibility	$C_f=5 \times 10^{-10}$	Pa^{-1}
Rock Compressibility	$C_r=5 \times 10^{-9}$	Pa^{-1}
Permeability	$k = 9.869\times10^{-13}$	m^2
Water Pumping Rate	$q_v = 0.1$	m^3/d
Wellbore Radius	$r_w = 0.1$	m
Outer Boundary Radius	$r_e = \infty \approx 5\times 10^6$	m
Dimensionless non-Darcy Flow Coefficient	$\beta_D = 1 \times 10^{-3}$, 1, 10, 100 1×10^3, 1×10^4, 1×10^5	

Table 2. Parameters for the single-phase, fractured-medium flow problem.

Parameter	Value	Unit
Matrix Porosity	$\phi_m = 0.30$	
Fracture Porosity	$\phi_f = 0.0006$	
Reference Water Density	$\rho_w = 1{,}000$	Kg/m^3
Water Phase Viscosity	$\mu_w = 1\times10^{-3}$	Pa•s
Matrix Permeability	$k_m = 1.0\times10^{-16}$	m^2
Fracture Permeability	$k_f = 9.869\times10^{-13}$	m^2
Water Production Rate	$q_m = 0.1$	kg/s
Rock Compressibility	$C_r = 1.0\times10^{-9}$	1/Pa
Water Compressibility	$C_w = 5.0\times10^{-10}$	1/Pa
Dimensionless non-Darcy Flow Coefficient for fracture	$\beta_{D,f} = 1 \times 10^{-4}$, 1, 5, and 10	
Dimensionless non-Darcy Flow Coefficient for matrix	$\beta_{D,m} = 1 \times 10^{-3}$, 10, 50, and 100	
Wellbore Radius	$r_w = 0.1$	m

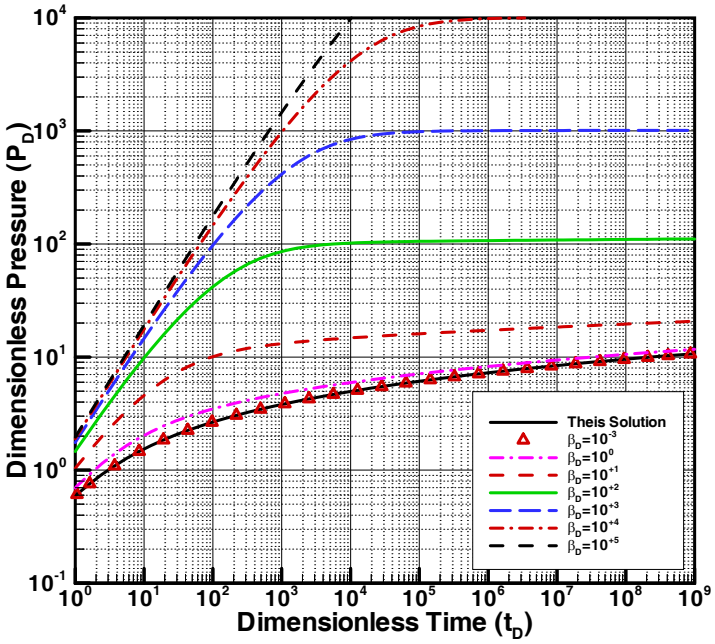

Figure 1. Type curves for dimensionless pressures for non-Darcy flow in an infinite system without wellbore storage and skin effects.

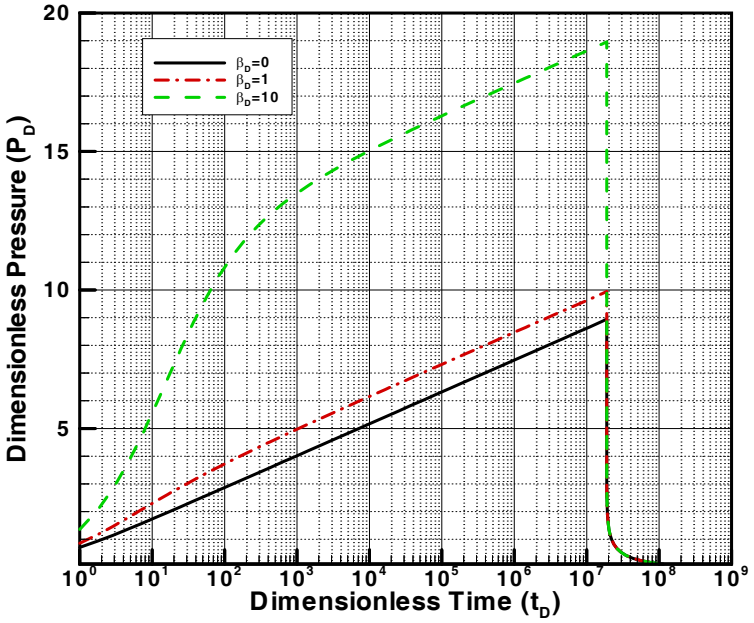

Figure 2. Dimensionless pressures for one-day pumping, followed by pressure buildup, of non-Darcy flow in an infinite system without wellbore storage and skin effects.

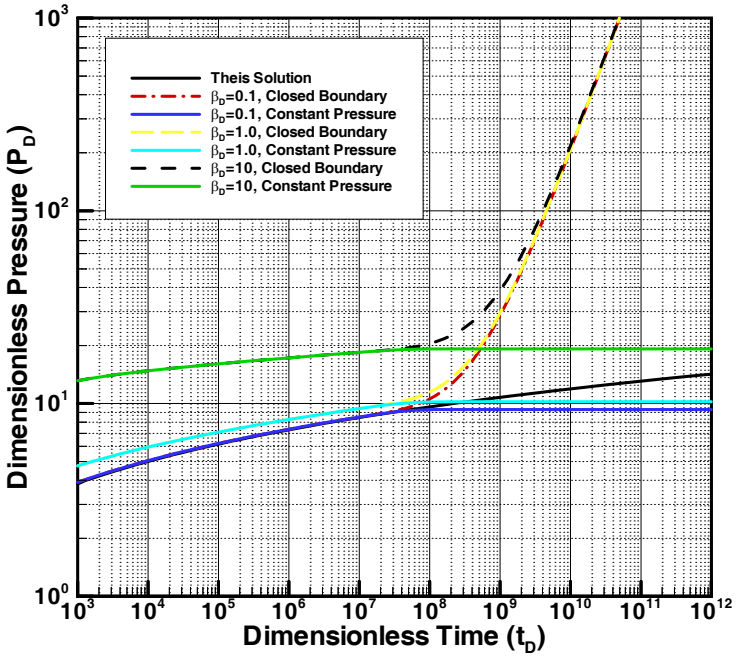

Figure 3. Type curves for dimensionless pressures for non-Darcy flow in a finite system with

an outer boundary radius of 1,000 m.

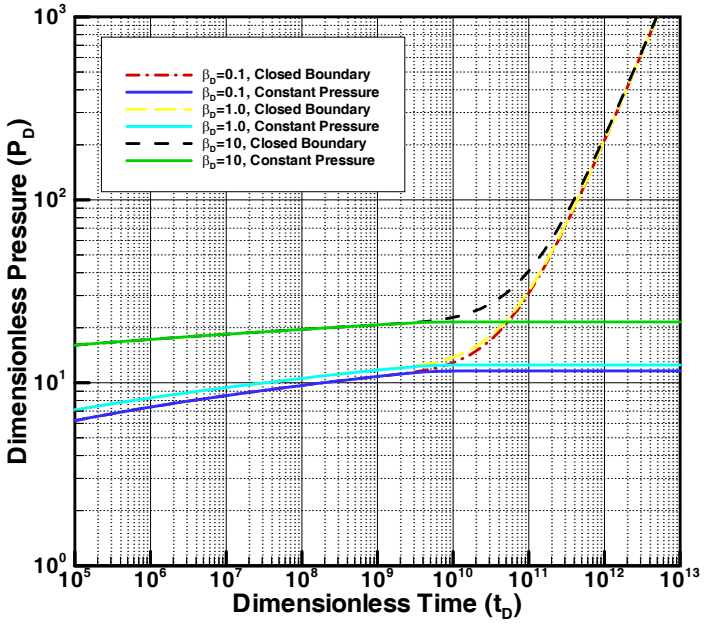

Figure 4. Type curves for dimensionless pressures for non-Darcy flow in a finite system with an outer boundary radius of 10,000 m.

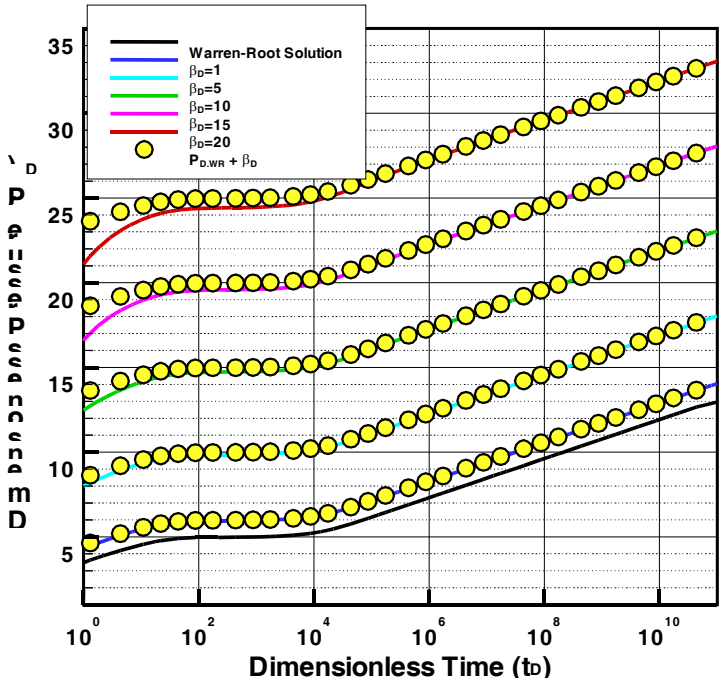

Figure 5 Type curves for dimensionless pressures for non-Darcy flow in an infinite fractured

system with comparisons with the approximate analytical solution.

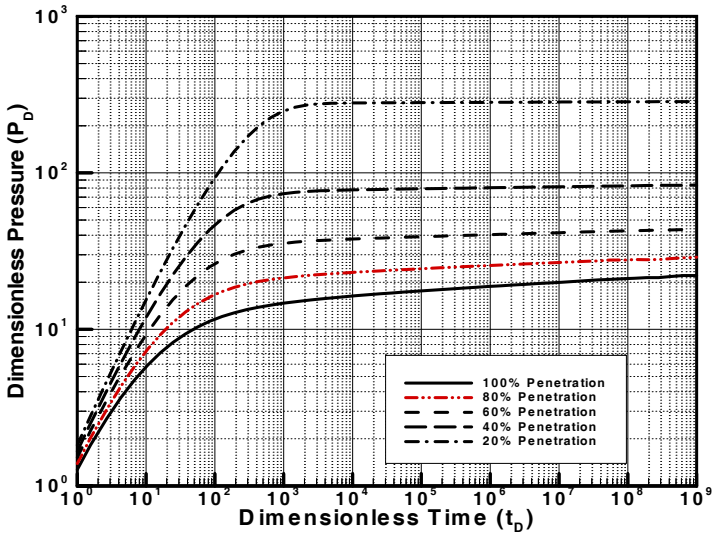

Figure 6. Type curves for dimensionless pressures of non-Darcy flow at partially penetrating wells in an infinite porous reservoir (β_D = 10) with different degrees of well penetration.

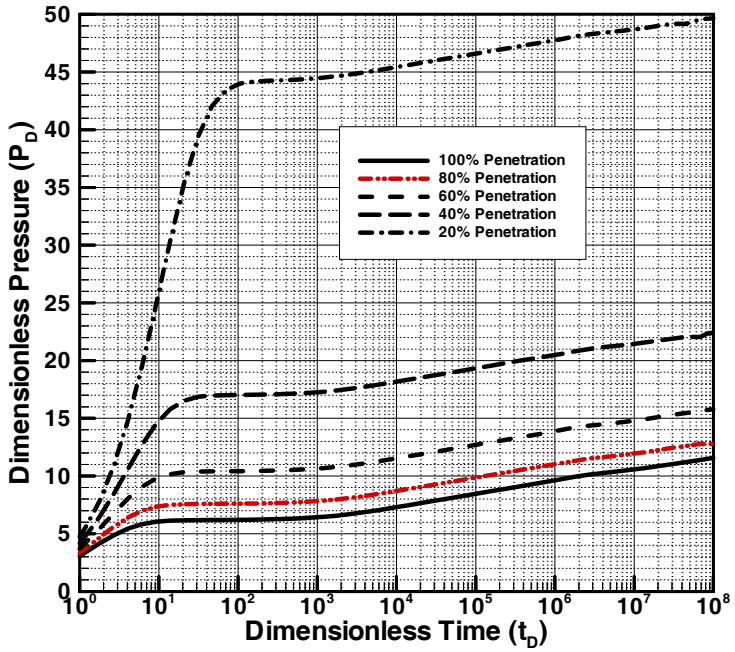

Figure 7. Type curves for dimensionless pressures of non-Darcy flow at partially penetrating wells in an infinite fractured reservoir (β_D = 1) with different degrees of well

penetration.